Detrimental copper-selenide bulk precipitation in CuIn1-xGaxSe2 thin-film solar cells. A possible reason for the limited performance at large x?

Polyxeni Tsoulka, Nicolas Barreau, Isabelle Braems, Ludovic Arzel, Sylvie Harel

▶ **To cite this version:**

Polyxeni Tsoulka, Nicolas Barreau, Isabelle Braems, Ludovic Arzel, Sylvie Harel. Detrimental copper-selenide bulk precipitation in CuIn1-xGaxSe2 thin-film solar cells. A possible reason for the limited performance at large x?. Thin Solid Films, 2020, 712, pp.138297. 10.1016/j.tsf.2020.138297 . hal-02945507

HAL Id: hal-02945507
https://hal.science/hal-02945507

Submitted on 25 Nov 2020

HAL is a multi-disciplinary open access archive for the deposit and dissemination of scientific research documents, whether they are published or not. The documents may come from teaching and research institutions in France or abroad, or from public or private research centers.

L'archive ouverte pluridisciplinaire **HAL**, est destinée au dépôt et à la diffusion de documents scientifiques de niveau recherche, publiés ou non, émanant des établissements d'enseignement et de recherche français ou étrangers, des laboratoires publics ou privés.

Detrimental copper-selenide bulk precipitation in $CuIn_{1-x}Ga_xSe_2$ thin-film solar cells. A possible reason for the limited performance at large x?

Polyxeni Tsoulka, Nicolas Barreau, Isabelle Braems, Ludovic Arzel, Sylvie Harel

Institut des Materiaux Jean Rouxel (IMN), UMR 6502 CNRS, Université de Nantes 2 rue de la Houssiniere BP 32229, 44322 Nantes cedex 3, France.

Abstract

In this paper, we propose a possible explanation of the limited $CuIn_{1-x}Ga_xSe_2$ (CIGSe) performance at high Ga contents, related to the properties of detrimental copper selenide ($Cu_\delta Se$) secondary phases. We study CIGSe layers at different x, by means of X-ray diffraction analyses, Raman and energy dispersive X-ray spectroscopy. Our results reveal that for high Ga contents, $Cu_\delta Se$ secondary phases either precipitate at the interfaces between grains or remain within the layer as intra- or inter-grain clusters, deteriorating the electronic properties of the absorber layer. On the contrary, for low Ga contents, the copper selenide segregates at the surface of the CIGSe and hence it can be easily removed by KCN surface etching. To understand the $Cu_\delta Se$ precipitation within the bulk of the film for a high Ga ratio, we also investigate In-free CGSe samples at low and high Cu content. Our observations demonstrate that i) $Cu_\delta Se$ has a preferential grain orientation to segregate and ii) the Cu-enriched regions within the bulk of the high Ga content films are more a kinetic than a thermodynamic issue.

Keywords: Copper indium gallium di-selenide; Thin films; Surface segregation; Bulk precipitation; Copper-selenium; Gallium ratio; Physical vapor deposition

1. Introduction

Polycrystalline $CuIn_{1-x}Ga_xSe_2$ (CIGSe) absorber layers count among the most promising materials in the field of thin-film solar cells. The CIGSe alloy can be described as a mixture of two ternary I-III-VI_2 semiconductors, $CuInSe_2$ (CISe) and $CuGaSe_2$ (CGSe), where the group III lattice sites are randomly occupied by In or Ga [1-3] and *x* corresponds to the Ga content:

$$x = \frac{[\mathrm{Ga}]}{[\mathrm{Ga}]+[\mathrm{In}]}$$

The optical band gap energy (E_g) of the absorber layer can be tuned by substituting Ga to In, from E_g=1.04eV for Ga-free CISe absorber layer (x=0) to 1.68 eV for In-free CGSe (x=1) [3,4].

In recent years, there has been considerable interest in the wide band gap materials like CGSe, since these absorber layers can be used *i*) to reach higher output voltage [4] and *ii*) as the top cell of a tandem stacked-type solar cell [5]. So far, the best lab-scale energy conversion efficiencies of CIG(S)Se-based solar cells are achieved for narrow band gap (23.35% for CIG(S)Se record efficiency [6]). Theoretically, the optimum Ga ratio to achieve the maximum conversion efficiency is around x~0.7 [7,8]. However, experimentally the efficiency of the CIGSe-based solar cells strongly decreases when *x* exceeds the threshold value of 0.4 [4-6,8].

The limited performance of Ga-rich (x>0.4) solar cells is under question for more than 25 years. The experimental and theoretical explanations behind the decreased photovoltaic performance at large *x* can be divided into two categories *i)* the detrimental recombination effects at CIGSe interfaces *i.e*. the CIGSe surface [9] and grain boundaries (GB) [10-12] and *ii)* the increased concentration of defects within the bulk of the film [4,13-15] that act as recombination centers.

Many experimental studies have shown that crystal defects [11,15,16], secondary phases and local inhomogeneities [17-20] can be created during the CIGSe deposition process at the inter- or intra-grain regions, *i.e.* segregation or precipitation phenomena at the grain boundaries or within the bulk. Cu-enriched regions or copper-selenide phases can be formed at the surface or/and within the bulk of the

CIGSe film at the inter- or intra-grain regions [11, 21-26]. The copper-selenide secondary phase possesses a semi-metallic character that enhance the charge transfer and acts as electron-hole recombination center. The excess of Cu at these regions increases the conductivity and creates an electric shunt. Hence, the electrical and optical properties of the absorber layer are negatively impacted [26-28], leading to the deterioration of the solar cell.

Copper-selenide secondary phases at the surface and at the inter-grain regions of the absorber layer have been observed in slightly Cu-rich CGSe layers by Kelvin probe force microscopy in [26] and by transmission electron microscopy (TEM) coupled with energy dispersive X-ray dispersion spectroscopy (EDS) in [27,29]. Additionally, studies of high-resolution scanning transmission electron microscopy (HR-STEM) on CIGSe layers [25] have shown the existence of copper-selenide inter- or intra-grain clusters. Further, a model based on Cu-poor and Cu-rich nanodomains creating a network has been proposed in [19,20].

In this paper, we focus on the formation of the detrimental Cu-enriched regions in the wide band gap CIGSe and CGSe compounds. We correlate the formation of the copper-selenide detrimental phase with the Ga ratio and we propose an approach that explains the degradation of the photovoltaic performance at large *x*.

The remainder of the paper is organized as follows:

Section 2 describes the co-evaporation process that we followed to synthetized the CIGSe and CGSe layers, the post-deposition treatments and the instruments that we used for our experimental analyses. Section 3.1 examines two CIGSe films of intermediate *x* and correlates the surface segregation and bulk precipitation phenomena of the copper-selenide with the Ga ratio. In Section 3.2, we study the copper selenide surface segregation mechanism and bulk precipitation in the case of In-free CGSe films at low and high Cu contents. Section 4 explains the observed copper selenide precipitation phenomena in the CIGSe layer from a kinetic point of view and proposes some directions for further research in order to

ameliorate the solar cell efficiency of the wide band gap CIGSe. Finally, the main conclusions of this study are drawn in Section 5.

2. Experimental

In our work, to investigate whether the Cu-enriched regions are related to the Ga content of the layer or not, we study the homogeneity of the absorber layer and the presence of the detrimental copper selenide phases in CIGSe layers of intermediate (x=0.3 and 0.6) and In-free (x=1) layers.

2.1 CIGSe co-evaporation process

In the present work, the absorber layers are synthesized by physical vapor deposition (PVD) process under vacuum (~10^{-4} Pa). During the CIGSe deposition process the flux (atoms per time unit) and the arrival rate per unit area of each element is controlled in order to obtain the desirable *i)* CIGSe thickness (1.5-2.0 μm), *ii)* Ga to In ratio (x) and *iii)* Cu to group-III atoms ratio (y):

$$y = \frac{[\mathrm{Cu}]}{[\mathrm{Ga}]+[\mathrm{In}]}$$

IR lamps were used as substrate heaters and the temperature was measured by a thermocouple in contact with the back of the substrate. To avoid a possible Ga gradient within the layer and focus only on the Cu diffusion, the Cu-RO process was chosen to synthesize the CIGSe films. The Cu-RO technique is a two-stage isothermal (T=560°C) process which starts with a Cu-Rich step (Stage I, y>1) and continues with a Cu-poor step (Stage II, y<1). The phase diagram of the ternary CISe compound [30, 31] shows that the chalcopyrite α-phase is stable from y=0.91 to 1 and that the homogeneous α-phase broadens with Na-doping and/or Ga to In substitution [32]. As regards the CGSe phase diagram [33, 34], the chalcopyrite phase is stable for y between 0.73 and 1. However, in both cases, the ternary phase diagrams reveal that for y>1 the chalcopyrite phase co-exists with the copper-selenide compounds ($CuSe_2$, CuSe, $Cu_{\delta}Se$). Hence, to keep the semiconductor character and avoid the presence of semi-metallic copper-selenide

secondary phases the final composition of the absorber layer is slightly Cu-poor (y<1). However, it should be noted that the thermodynamic equilibrium may not be reached during the CIGSe deposition process and hence the presence of secondary phases, such as the detrimental copper-selenides. During the whole co-evaporation process the Se flux is in excess and the overall deposition rate is 30 nm/min. More details about the Cu-RO co-evaporation technique can be found in [35]. A single-stage co-evaporation process at 560°C substrate temperature was also carried out to study separately the case of a Cu-rich CGSe layer.

The CIGSe layers of intermediate x were deposited on soda-lime glass (SLG)/Si_xN/Mo substrate at 560°C. The Si_xN layer serves as an alkali diffusion barrier. Studies have shown that Na diffusion within the CIGSe layer, hinders the In-Ga interdiffusion [36, 37, 38]. Hence, to avoid any possible Ga grading within the CIGSe layers of intermediate x, the absorbers were co-evaporated on soda-lime glass (SLG)/Na-barrier(Si_xN)/Mo substrate. The In-free CGSe layers were deposited on standard SLG/Mo substrates.

2.2 Post-deposition treatments

After the end of the co-evaporation process, we applied a wet-chemical etching of the CIGSe surface using a potassium cyanide (KCN) solution [39] in order to remove any possible surface segregated Cu-rich secondary phases. Here, we should notice that the KCN etching removes only the copper selenides from the surface, without acting on any possible Cu-rich compound in the bulk or the inter-grain regions of the CIGSe film [26-28]. Finally, after the KCN etching some of the samples were annealed under vacuum at 350°C for 24h or 30 days in order to reach the thermodynamic equilibrium and avoid the presence of secondary phases. Table I summarizes the samples that we used in our study.

2.3 Characterization

The composition of the CIGSe layer was measured by EDS coupled with a SEM (scanning electron microscope) using a JEOL JSM 5800LV at 5 kV (surface analysis) and 20 kV (bulk analysis) acceleration voltage. In-line cross-section elemental profile was also performed on one of our samples (#04) using SEM-EDS at 10 kV acceleration voltage. The cross-section analyzed area was mechanically polished using the ultramicrotome Leica UC7 equipped with a diamond knife. For the high resolution SEM images a JEOL JSM 7600F microscope was used.

Raman spectroscopy was applied for the chemical analysis of the near surface region of the CIGSe layers (surface analysis). The system used is a Renishaw InVia Reflex and the wavelength of the excitation beam was set to 488 nm using an Ar^+ laser source. The interaction depth at 488 nm excitation wavelength corresponds to less than 150 nm.

The structural observation of the CIGSe films was based on an XRD (X-ray diffraction) study, with a Siemens D8 integrated with a Cu-Ka source radiation (λ=1.54056 Å).

3. Results

3.1 Copper selenide precipitation phenomena in CIGSe layers of intermediate *x*

In the present section, we study the samples of intermediate Ga content (sample #01 with x=0.30 and #02 with x=0.60) and the creation of Cu-enriched local inhomogeneities within the bulk of the CIGSe layers.

The CIGSe layers were deposited on SLG/Si_xN/Mo using the Cu-RO process. After the end of the co-evaporation process, the samples were KCN-etched, sealed under vacuum in a quartz tube and annealed at 350°C for 30 days.

- **Surface morphology**

The CIGSe surface morphology of the samples without any post deposition treatment is shown in Figure 1. The Sample #02 (x=0.60) presents a rough surface and an important amount of grains with a

triangular morphology. According to [40,41] the faceted grains are {112}-oriented and the ledges of the triangles correspond to {220}/{204} planes. The x=0.30 samples present a smoother surface than the x=0.60 ones. Figure 2 gives a high-magnification SEM image of the surface after the KCN treatment and the annealing.

On the x=0.30 annealed sample, we observe the existence of voids at the surface which are created by the removal of the copper-selenide phases after the KCN surface etching. This observation is in line with the EDS analysis (see table I), which shows that after the KCN treatment and annealing, the overall Cu content is decreased from y=0.98 to 0.92, due to the copper-selenide removal after the KCN etching. In contrast, on the CIGSe x=0.60 annealed sample the Cu content did not significantly change (from y=0.87 to 0.86) after the KCN treatment and the annealing. Moreover, in Figure 2 we can see small clusters aligned along precise orientations of grains having the ledge-patterned morphology.

- **Copper selenide surface segregation in CIGSe of intermediate *x***

To identify the probable existence of different phases at the surface of the CIGSe film and investigate the chemical composition of the ledge-patterned grains containing the clusters, we performed a Raman analysis (see Fig. 3) at the upper CIGSe layers. The Raman peak at 175 cm^{-1} for the x=0.30 CIGSe film and at 179 cm^{-1} for 0.60 is related to the main A_1 CIGSe vibration mode [42, 43] of the Se anions. The two spectra also depict the weak B_2/E stretching In/Ga-Se mode [42, 43] around 216 cm^{-1} and 239 cm^{-1} for x=0.30 and around 226 cm^{-1} and 242 cm^{-1} for x=0.60. The shift of chalcopyrite peaks at larger wavenumber, observed for x=0.60, is due to the decrease of the lattice parameters [44] of the high Ga content crystals. The additional peak at 259 cm^{-1} corresponds to the A_1 vibration mode of a copper-selenide compound as the CuSe, Cu_2Se or $Cu_{2-\delta}Se$, according to [42, 43, 45]. Moreover, our results show that after the end of the co-evaporation process both samples exhibit a copper-selenide phase at the surface, while after the KCN chemical etching and the annealing only the Ga-rich (x=0.60) sample

presents a copper-selenide phase at the surface. In the In-rich sample there is no Cu-Se Raman peak after the post-deposition KCN treatment and the annealing.

Comparing the black lines in Figures 3a and 3b, we notice that prior to the KCN etching and the annealing, the intensity of the $Cu_{\delta}Se$ peak is more pronounced for the sample with x=0.60 than for the one with x=0.30, indicating a larger Cu content. This observation could be related with the smoother surface observed for x=0.30 (see Fig. 1).

The red lines correspond to the Raman spectra after the KCN treatment and the annealing. Within the x=0.30 all the $Cu_{\delta}Se$ was removed from the CIGSe surface after the KCN etching and no further $Cu_{\delta}Se$ accumulation was observed at the CIGSe upper layers after the annealing. In contrast, the x=0.60 KCN treated and annealed sample presents a $Cu_{\delta}Se$ compound at the surface after the annealing, which could be related with the aligned clusters observed at the CIGSe surface after the annealing (Fig. 2) as mentioned above.

Thus, comparing the x=0.60 (Ga-rich CIGSe) Raman spectra before and after the post deposition treatment, it can be assumed that there are $Cu_{\delta}Se$ precipitates in the bulk of the Ga-rich (x=0.60) layer after the end of the CIGSe co-evaporation process and the KCN etching. Hence, after the annealing where the thermodynamic equilibrium has been reached, the bulk-precipitated $Cu_{\delta}Se$ segregates at the surface. Thus, the copper selenide peak in Raman spectra after the post deposition treatment corresponds to the $Cu_{\delta}Se$ phase that has segregated at the surface after the annealing. In contrast this is not the case for x=0.30 (In-rich CIGSe), since there is no $Cu_{\delta}Se$ peak in the Raman spectra after the KCN treatment and the annealing, indicating that all the $Cu_{\delta}Se$ was segregated at the surface after the end of the co-evaporation process, and removed afterwards by the KCN treatment. Hence, no $Cu_{\delta}Se$ remained trapped in the bulk of the film after the CIGSe deposition process.

- **CIGSe texture**

The XRD diffractograms (Fig. 4) do not show any copper selenide peak and the only identified phase is the chalcopyrite. This raises questions about the $Cu_{\delta}Se$ form within the bulk, since it could be present as an amorphous phase at the inter- or intra-grain region or as small crystallites that cannot be detected with the XRD analysis.

The diffractograms show that the CIGSe layers are mainly (112)-oriented (peak at 26.9° for x=0.30 and at 27.2° for x=0.60) and none of the samples presents a peak related to a copper-selenide phase. The shift of the (112) peak to higher angles for x=0.60 indicates that the lattice parameters are decreased compared to x=0.30. In our case the resulting (112) preferential orientation strongly depends on the high isothermal deposition temperature and the texture of the Cu-rich precursor layer, where the cubic Cu_2Se and tetragonal non-stoichiometric $Cu_{\delta}Se$ phases are (111)-oriented.

Examining the samples before and after annealing reveals that the full width at half maximum (FWHM) of the (112) orientation is decreasing after the annealing ($FWHM(112)_{before}$ - $FWHM(112)_{after}$ = 0.01°) which indicates a grain size enlargement.

Proposed scenario: Detrimental copper-selenide bulk precipitation at large *x*

The comparison between the x=0.30 and x=0.60 XRD and Raman data leads us to conclude that the Cu-Se segregation phenomena differ for low and high Ga ratios: in the Ga-rich sample there are $Cu_{\delta}Se$ precipitates within the bulk after the end of the co-evaporation process, contrary to the In-rich sample where the whole $Cu_{\delta}Se$ has segregated at the surface. A longer annealing is then required for x=0.60 to make the entire $Cu_{\delta}Se$ segregate at the surface. In addition the fact that no $(In,Ga)_2Se_3$ or other Cu-poor phases (i.e. $Cu(In,Ga)_3Se_5$) were observed after the annealing, reveals that copper selenide compounds observed at the surface after the annealing came from the bulk and no $(In,Ga)_2Se_3$-Cu_2Se phase separation occurred during the annealing. Figure 5 presents a schematic model of $Cu_{\delta}Se$ behavior in the case of low (x=0.30) and high (x=0.60) Ga content, before and after the post-deposition treatment.

3.2 Bulk precipitation and surface segregation phenomena in $CuGaSe_2$

To further understand the cause of the copper-selenide bulk precipitation observed in CIGSe layers with large Ga ratios, we focus on In-free CGSe layers with high and low Cu content and we investigate the $Cu_{\delta}Se$ segregation mechanism and the crystallinity of the copper-selenide compounds at the surface and within the layer.

- **$Cu_{\delta}Se$ surface segregation via a precise grain orientation**

To study the $Cu_{\delta}Se$ surface segregation in the case of high Ga contents, we perform a surface SEM-EDS cartography on a Cu-rich (y>1) CGSe sample (#03) before and after annealing. The layer was deposited using a single-stage process, resulting in a final CGSe layer with y=1.50. After the end of the deposition process the sample was annealed for 24h at 350°C under vacuum.

Figure 6 shows SEM images of the Cu-rich surface before and after the annealing. As shown in Figure 6a, the surface of the sample before annealing presents two main types of grains: *i)* smooth single faceted grains and *ii)* rough grains where periodic steps create a ledged patterned surface. In the surface of the annealed sample (Fig. 6b and 6c) small clusters accumulate at the ledges of the rough grains. Recall that the same phenomenon was observed for the Ga-rich sample (see Fig. 2 in Section 3.1).

Further an EDS cartography was carried out at 5 kV acceleration voltage, in order to decrease the interaction depth of the electron beam and be able to analyze only the upper layers of the surface. Using the Casino software [46], we carried out a Monte Carlo simulation (not shown here) of the interaction volume of our SEM-EDS analysis at 5 kV beam energy and we found that the interaction depth is around 150 nm. The EDS cartography (see Fig. 7) revealed that the upper layers of the grains containing the clusters on their surface are Cu-rich. Thus, we conclude that the $Cu_{\delta}Se$ has a preferential grain orientation to segregate, since after the annealing, it accumulates only at the ledges of the {112}-oriented grains with the precise step-patterned surface.

- **Crystallinity of the bulk-precipitated $Cu_{\delta}Se$ phase**

Here, we examine the presence of Cu-rich regions within the layer of slightly Cu-poor CGSe samples and we investigate the $Cu_{\delta}Se$ form in the bulk. The CGSe samples were synthesized by a two-stage (Cu-RO) co-evaporation process on Mo (#04, y=0.95) the sample was chemically etched with KCN after the end of the deposition process. Figure 8 depicts the XRD diffractogram of the CGSe sample (#04) with y=0.95 grown on Mo and no peak of $Cu_{\delta}Se$ is apparently observed. However, the in-line cross-section elemental profile, using a SEM-EDS at 10 kV acceleration voltage (Fig. 9), presents a small variation of the Cu content, resulting in a slight Cu-rich region close to the back contact. The fact that the XRD analysis of the sample did not indicate any $Cu_{\delta}Se$ peak, while the EDS cross-section profile detects a Cu-rich region, leads us to the conclusion that the $Cu_{\delta}Se$ precipitates in the bulk are present in an amorphous form. However, this assumption does not exclude a possible $Cu_{\delta}Se$ precipitation at the inter-grain regions or the existence of small not-detectable crystallites within the grains.

4. Discussion

In this paper, we examined the copper-selenide precipitation and the presence of Cu-rich secondary phases in regard to the Ga content of the thin films. Our investigations suggest that for large Ga ratios (x> 0.4), copper-selenide compounds precipitate within the bulk of the film or/and close to the back contact, whereas for low Ga contents the whole undiluted $Cu_{\delta}Se$ segregates at the surface. This is a vital issue for future research in the wide band gap CIGSe absorber layers since the Cu-rich regions within the bulk could be a possible explanation of the observed photovoltaic degradation at large Ga contents (when x>0.4).

Our observations are consistent with the findings in [19] where the cubic Cu_2Se phase was observed by TEM-EDS micro-analysis, on the CIGSe surface and the $Cu_{2-\delta}Se$ tetragonal phase at the interface between the grains. Additionally, in [11] an atom probe tomography (APT) analysis on CIGSe revealed the presence of Cu-enriched grain boundaries when x>0.8 and In-enriched GBs for x<0.4.

Our studies have also shown that the copper selenide is facilitated by a precise orientation of the grains. This observation could be correlated with the findings in [25], where studies of HR-STEM and electron energy-loss spectroscopy revealed the presence of platelets of copper selenides within the grains, parallel to the {112} planes of the CIGSe.

An interesting question to address is how is it possible to have Cu-enriched regions in a stoichiometric or slightly Cu-poor (y<1) film of large Ga content, since according to the CISe, CGSe and CIGSe [30-34, 47, 48] phase diagrams the copper selenide phase is formed and co-exists with the chalcopyrite phase only when y>1. For y<1 there is only the co-existence of Cu-poor CIGSe compositions with the chalcopyrite phase. Taking into account, that *i)* during the deposition process we are not under thermodynamic equilibrium and *ii)* the CISe and CGSe kinetic properties differ [38,49-51], we can assume the creation of local inhomogeneities during the CIGSe formation. Moreover, of particular interest is the fact that only in the case of Ga-rich film a long annealing is needed to make the copper-selenide segregate at the surface.

In contrast, for the In-rich CIGSe synthesis, the duration of the deposition process is sufficient to make the excess of copper segregate at the surface, resulting in a homogeneous and close to stoichiometry bulk composition of the film. The same result is also observed in the In-free CGSe layer of y>1 where segregated clusters are observed at the step-patterned grains after an annealing of 24 hours. Hence, the Cu-rich precipitates within the bulk of the Ga-rich films is more a kinetic than a thermodynamic issue. As highlighted in our previous paper [52] for the CGSe wide band gap solar cells, applying two annealing stages during the 3-stage (Cu Poor-Rich-Off) process results in an improved lateral uniformity of the metal atoms and better solar cell device performance (the current density is increased by 11.2% and the solar cell efficiency by 8% . In [52] the Raman analysis at the front and rear surface of CGSe samples with and without annealing stages show that the absorber synthesized without any annealing step presents a nonuniform Cu/Ga distribution and higher amount of Cu at the rear surface, while the

CGSe sample synthesized with two relaxation stages during the growth exhibits homogeneous Cu/Ga distribution. Similarly, another previous study [53] on CGSe samples grown with and without relaxation stages by a Cu-RO process and analyzed by Raman spectroscopy at the front and rear CGSe surface indicate an improved homogeneity and solar cell efficiency when the relaxation stage is applied during the growth.

Considering *i)* the different electronegativity between Ga and In, *ii)* the structural CIGSe variation with the Ga content (*x*) and *iii)* the different reaction pathways and reaction speed of the two pure ternary compounds [38, 50, 51], it can be assumed that different precipitation and segregation phenomena will take place at low and high *x*. Taking into account previous studies on the thermodynamic and kinetic properties of CISe and CGSe, it appears more probable to have local inhomogeneities and secondary Cu-rich phases in the case of high Ga contents, since:

i) The reaction rates of CISe and CGSe are different, CGSe being formed much slower than CISe at a given temperature [49, 54]. In fact, in [49, 54], studies on the formation rates of CISe and CGSe by selenization of Cu/In and Cu/Ga precursors, respectively, demonstrated that the time to form CGSe by selenization of a Cu/Ga precursor at 500°C is six times larger than the formation of CISe [49] and that at 400°C the CISe needs 30 min to be formed when CGSe needs 90 min at 450°C [52].

ii) Studies of the CGSe and CISe reaction kinetics using isothermal soak of glass/GaSe/CuSe and glass/InSe/CuSe precursors, show that the activation energy of the CGSe formation is larger than the activation energy of CISe (115 kJ/mol and 66 kJ/mol, respectively) [50, 51].

Hence, given that the Cu-enriched regions within the bulk of the Ga-rich layer are a kinetic issue and the copper selenide surface segregation takes place via a precise orientation of the grains, special attention should be taken to the deposition process for Ga-rich CIGSe layers in order to:

a) Control the texture of the CIGSe film.

Studies on the CIGSe deposition process have shown that the preferential orientation of the CIGSe films depends on: a) the alkali impurities such as K and Na, that diffuse via the SLG substrate [55-59] b) the Se flux during the co-evaporation process [40, 58-60], c) the deposition temperature [56, 57, 59] and d) Cu concentration [56, 57, 61].

b) Enhance the interdiffusion of the elements in order to obtain a more homogeneous absorber layer.

The presence of a high amount of Ga in the CIGSe lattice seems to weaken the interdiffusion of elements and so it could be responsible for the creation of secondary intra-grain phases as the $Cu_{\delta}Se$. In [8], it was observed that for $0.3 < x < 1$, the CIGSe films presented higher efficiencies for substrate temperatures higher (600°C-650°C) than the commonly used ones (500°C-600°C).

Additionally, attention should be paid on the fact that the annealing of our samples was performed under vacuum. As a result, the observed grain enlargement and homogenization of the film could be also related with the increased amount of Se vacancies that could act as diffusion pathways [54, 62].

5. Conclusions

In this paper, we developed an approach to understand the copper selenide behavior in the CIGSe layer at low and high Ga content. We studied CIGSe samples at intermediate x (0.3 and 0.6) and at low (y<1) and high (y >1) Cu content. Our work revealed that the copper selenide segregation phenomena depend on the Ga ratio. We demonstrated that for large Ga content there are Cu-enriched detrimental precipitates within the bulk of the layer, while for low Ga ratio the whole copper selenide segregates at the surface and then can be easily removed by KCN wet-chemical etching.

We also investigated pure CGSe layers at low and high Cu contents grown on SLG/Mo. We concluded that the Cu-enriched regions within the bulk of the Ga-rich layer are a kinetic issue and the copper selenide surface segregation mainly occurs via a precise orientation of the grains.

Considering that the $Cu_{\delta}Se$ compounds have a metallic character which degrades the electrical properties of the solar cell, our findings could be a possible explanation for the limited photovoltaic performance at high Ga contents. Hence, the copper selenide secondary phases in the CIGSe layer are an important issue for future research.

What is known about the $Cu_{\delta}Se$ in the CIGSe field is largely based on narrow band gap CIGSe ($x < 0.4$) and so, further investigation on the $Cu_{\delta}Se$ formation at the Ga-rich CIGSe layers is required. In addition, a re-investigation of the co-evaporation processes should be considered, since for large Ga ratios, the excess of Cu during the Cu-rich stage seems to create Cu-enriched regions within the bulk, which are not diluted or segregated at the surface during the Cu-poor co-evaporation step. Nevertheless, the Cu-rich deposition stage is essential for a high quality CIGSe absorber layer, since during this step the mobility and the interdiffusion of the elements is increased, facilitating the grain growth [61].

Taken together, the results of our study suggest that the deposition process should be adapted to the needs of the wide band gap CIGSe and CGSe absorbers. To improve the quality of the wide bad gap CIGSe absorbers and obtain high-efficiency solar cells, it is important to: *i)* keep the Cu content as close as possible to stoichiometry (y=1), during the Cu-rich co-evaporation step, *ii)* control the texture of the CIGSe layer, *iii)* increase the diffusion pathways by decreasing the Se flux during the process and *iv)* increase the deposition temperature or/and the duration of the process by adding a relaxation stage or by decreasing the deposition rate, in order to enhance the Cu-Ga interdiffusion.

Acknowledgments

This work was supported by the Jean Rouxel Institute of materials and the University of Nantes. We gratefully acknowledge Prof. Angus Rockett, who gave us much valuable advice at the beginning of this work. Thanks is due to Nicolas Stephant and Nicolas Gautier for their technical assistance in our experimental work.

References

[1] J.E. Jaffe, A. Zunger, Electronic structure of the ternary chalcopyrite semiconductors $CuAlS_2$, $CuGaS_2$, $CuInS_2$, $CuAlSe_2$, $CuGaSe_2$, and $CuInSe_2$, Phys. Rev. B 28 (1983) 5822-5847

[2] C. Stephan, Structural trends in off stoichiometric chalcopyrite type compound semiconductors, PhD Thesis, Berlin (2011)

[3] T. Tinoco, C. Rincón, M. Quintero, G.S. Pérez, Phase diagram and optical energy gaps for $CuIn_yGa_{1-y}Se_2$ alloys, Phys. Status Solidi (a) 124 (1991) 427–434

[4] S.-H. Wei, S.B. Zhang, A. Zunger, Effects of Ga addition to $CuInSe_2$ on its electronic, structural, and defect properties, Appl. Phys. Lett. 72 (1998) 3199-3201

[5] S. Nishiwaki, S. Siebentritt, P. Walk, M.Ch. Lux-Steiner, A stacked chalcopyrite thin-film tandem solar cell with 1.2V open-circuit voltage, Prog. Photovoltaics Res. Appl. 11 (2003) 243-248

[6] http://www.solar-frontier.com/eng/news/2019/0117_press.html

[7] W. Shockley, H.J. Queisser, Detailed balance limit of efficiency of p-n junction solar cells, J. Appl. Phys. 32 (1961) 510-519

[8] M.A. Contreras, L.M. Mansfield, B. Egaas, J. Li, M. Romero, R. Noufi, E. Rudiger-Voigt, W. Mannstadt, Wide bandgap $Cu(In,Ga)Se_2$ solar cells with improved energy conversion efficiency, Progr. Photovolt: Res. Appl. 20 (2012) 843–850

[9] M. Saad, A. Kassis, Thermally and light-activated current in $ZnO/CdS/CuGaSe_2$ single crystal solar cells, Renew. Energy 33 (2008) 974-978

[10] H. Mirhosseini, J. Kiss, C. Felser, Behavior of Σ3 grain boundaries in $CuInSe_2$ and $CuGaSe_2$ photovoltaic absorbers revealed by first-principles hybrid functional calculations, Phys. Rev. Appl. 4 (2015) 1-6

[11] M. Raghuwanshi, Influence of grain boundary chemistry on the properties of CIGS photovoltaic cells, PhD Thesis, Rouen (2015)

[12] C.-S. Jiang, R. Noufi, K. Ramanathan, J.A. AbuShama, H.R. Moutinho, M.M. Al Jassim, Local built-in potential on grain boundary of $Cu(In,Ga)Se_2$ thin films, Renew. Energy 1 (2005) 245-246

[13] J.T. Heath, J. D. Cohen, W.N. Shafarman, D. X. Liao, A.A. Rockett, Effect of Ga content on defect states in $CuIn_{1-x}Ga_xSe_2$ photovoltaic devices, Appl. Phys. Lett. 80 (2002) 4540-4542

[14] A. Darga, W. Favre, M. Fruzzetti, J.-P. Kleider, B. Morel, D. Mencaraglia, P.Yu, H. Marko, L. Arzel, N. Barreau, S. Noël, J. Kessler, Study of the electronic properties of wide band gap CIGSe solar cells: Influence of copper, J. Non Cryst. Solids 358 (2012) 2428-2430

[15] S. Lany, A. Zunger, Limitation of the open-circuit voltage due to metastable intrinsic defects in $Cu(In,Ga)Se_2$ and strategies to avoid these defects, Preprint. Renew. Energy (2008) 7-9

[16] S. B. Zhang, S.-H. Wei, A. Zunger, H. Katayama-Yoshida, Defect physics of the $CuInSe_2$ chalcopyrite semiconductor, Phys. Rev. B - Condens. Matte. Phys. 57 (1998) 9642-9656

[17] U. Rau, J.H. Werner, Radiative efficiency limits of solar cells with lateral band-gap fluctuations, Appl. Phys. Lett. 84 (2004) 3735-3737

[18] J.R. Tuttle, D.S. Albin, R. Noufi, Thoughts on the microstructure of polycrystalline thin film $CuInSe_2$ and its impact on material and device performance, Sol. Cells 30 (1991) 21-38

[19] R. Noufi, Y. Yan, J. Abu-Shama, K. Jones, M. Al-Jassim, B. Keyes, J. Alleman, K. Ramanathan, Investigation of the microstructure of $Cu(In,Ga)Se_2$ thin films used in high-efficiency devices, Preprint Renew. Energy (2002) 1-4

[20] Y. Yan, R. Noufi, K.M. Jones, K. Ramanathan, M.M. Al-Jassim, B.J. Stanbery, Chemical fluctuation-induced nanodomains in $Cu(In,Ga)Se_2$ films, Appl. Phys. Lett. 87 (2005) 1-3

[21] T. Wada, N. Kohara, T. Negami, M. Nishitani, Growth of CuinSe$_2$ crystals in Cu-rich Cu-In-Se thin films, J. Mater. Res. 12 (1997) 1456-1462

[22] D. Abou-Ras, S.S. Schmidt, R. Caballero, T. Unold, H-W. Schock, C.T. Koch, B. Schaffer, M. Schaffer, P.-P. Choi, O. Cojocaru-Mirédin, Confined and chemically flexible grain boundaries in polycrystalline compound semiconductors, Adv. Energy Mater. 2 (2012) 992-998

[23] E. Simsek Sanli, Q.M. Ramasse, W. Sigle, D. Abou-Ras, R. Mainz, A. Weber, H.-J. Kleebe, P. A. van Aken, Elemental redistributions at structural defects in Cu(In,Ga)Se$_2$ thin films for solar cells, J. Appl. Phys. 120 (2016) 205301

[24] T. Schwarz, G. Stechmann, B. Gault, O. Cojocaru-Miredin, R. Wuerz, D. Raabe, Correlative transmission Kikuchi diffraction and atom probe tomography study of Cu(In,Ga)Se$_2$ grain boundaries Prog. Photovolt. Res. Appl. (2017) 1-9

[25] E. Simsek Sanli, Q.M. Ramasse, R. Mainz, A. Weber, D. Abou-Ras, W. Sigle, P.A. van Aken, Evidence for $Cu_{2-x}Se$ platelets at grain boundaries and within grains in Cu(In,Ga)Se$_2$ thin films, Appl. Phys. Lett. 111 (2017) 32103

[26] D.F. Marron, Th. Glatzel, A. Meeder, Th. Schedel-Niedrig, S. Sadewasser, M.Ch. Lux-Steiner, Electronic structure of secondary phases in Cu-rich CuGaSe$_2$ solar cell devices, Appl. Phys. Lett. 85 (2004) 3755-3757

[27] D.F. Marron, A. Meeder, U. Bloeck, P. Schubert-Bischoff, N. Pfander, R Wurz, S. M.Babu, Th. Schedel-Niedrig, M.Ch. Lux-Steiner, Microstructural properties of CVD-grown CuGaSe$_2$ based thin film solar cells, Thin Solid Films 431–432 (2003) 237-341

[28] H. Marko, L. Arzel, A. Darga, N. Barreau, S. Noël, D. Mencaraglia, J. Kessler, Influence of Cu off-stoichiometry on wide band gap CIGSe solar cells, Thin solid films 519 (2011) 7228-7231

[29] S. Nishiwaki, S. Siebentritt, M. Giersig, M.Ch. Lux-Steiner, Growth model of grains in a Cu-rich/Cu-poor bilayer process, J. Appl. Phys. 94 (2003) 6864-6870

[30] T. Godecke, T. Haalboom, F. Ernst, Phase equilibria of Cu-In-Se. I Stable states and equilibrium stats of the In_2Se_3-Cu_2Se system, Z Metallkd 91 (8) (2000) 622-634

[31] T. Haalboom, T. Gödecke, F. Ernst, M. Rühle, R. Herberholz, H. W. Schock, C. Berlharz, K. W.Berz, Phase relations and microstructure in bulk materials and thin film of ternary system Cu-In-Cu, Proceedings of the Int. Conf. on Ternary and Multinary Compounds, Inst. Phys. Conf. ser. No 152: Section B: Thin Film Growth and Characterization (1997) 249-252

[32] R. Herberholz, U. Rau, H. W. Schock, T. Haalboom, T. Gödecke, F. Ernst, C. Beilharz, K. W. Benz, D. Cahen, Phase segregation, Cu migration and junction formation in Cu(In,Ga)Se_2, Eur. Phys. J. AP 6 (1999) 131-139

[33] L. S. Palatnik, E. K. Belova, Atroshch.Lv and Y. F. Komnik, Sov Phys Crystallogr 10 (4) (1966) 395

[34] J.C. Mikkelson, Ternary phase relations of the chalcopyrite compound $CuGaSe_2$, J. Electron. Mater. 10 **(**1981**)** 541-558

[35] J. Kessler, J. Schöldström, L. Stolt, Rapid Cu(ln,Ga)Se_2 growth using "End Point Detection", Conf. Rec. IEEE Photovolt. Spec. conf. 2000-January (2000) 509-512

[36] O. Lundberg, J. Lu, A. Rockett, M. Edoff, L. Stolt, Diffusion of indium and gallium in Cu(In,Ga)Se_2 thin film solar cells, J. Phys. Chem. Solids 64 (2003) 1499-1504

[37] B. Namnuan, K. Yoodee, S. Chatraphorn, Probig diffusion of In and Ga in $CuInSe_2$/$CuGaSe_2$ bilayer thin films by X-ray diffraction, J Crys. Growth 432 (2015) 24-32

[38] F. Hergert, S. Jost, R. Hock, M. Purwins, A crystallographic description of experimentally identified formation reactions of Cu(In,Ga)Se_2, J. Solid State Chem. 179 (2006) 2394-2415

[39] J. Lehmann, S. Lehmann, I. Lauermann, T. Rissom, C.A. Kaufmann, M. Ch. Lux-Steiner, M. Bär, S. Sadewasser, Reliable wet-chemical cleaning of natively oxidized high-efficiency Cu(In,Ga)Se_2 thin film solar cell absorbers, J. Appl. Phys. 116 (2014) 233502

[40] K.H Kim, K.H. Yoon, J.H Yun, B.T. Ahn, Effects of Se flux on the microstructure of Cu(In,Ga)Se_2 thin film deposited by a three-stage co-evaporation process, Electrochem. Solid-State Lett. 9 (2006) 382-384

[41] A. Rockett, Surface analysis of chalcopyrite materials for photovoltaics, Progr. Photovolt. Res. Appl. 20 (2012) 575-581

[42] D. Papadimitriou, N. Esser, C. Xue, Structural properties of chalcopyrite thin films studied by Raman spectroscopy, Phys. Status Solidi 242 (2005) 2633-2643

[43] W. Witte, R. Kniese, M. Powalla, Raman investigations of Cu(In,Ga)Se_2 thin films with various copper contents, Thin solid Films 517 (2008) 867-569

[44] W. Witte, R. Kniese, A. Eicke, M. Pawolla, Influence of Ga content on the Mo/Cu(In,Ga)Se_2 interface formation, 2006 IEEE 4^{th} World Conference on Photovoltaic Energy Conference, Waikoloa, HI, (2006) 553-556

[45] C. Xue, D. Papadimitriou, Y.S. Raptis, W. Richter, N. Esser, S. Siebentritt, M. Ch. Lux-Steiner, Micro-Raman Study of Orientation Effects of Crystallites on Cu-rich Thin Films, J. Appl. Phys. 96, (2004) 1963-1966

[46] D. Drouin, A.R. Couture, D. Joly, X. Tastet, V. Aimez, R. Gauvin, CASINO V2.42—A fast and Easy-to-use modeling tool for scanning electron Microscopy and microanalysis Users, Scanning 29 (2007) 92-101

[47] T. Maeda, W. Gong, T. Wada, Crystallographic and optical properties and band structures of $CuInSe_2$, $CuIn_3Se_5$, and $CuIn_5Se_8$ phases in Cu-poor Cu_2Se–In_2Se_3 pseudo-binary system J. Appl. Phys. 55 **(**2016) 04ES15

[48] C. Beilharz, Charakterisierung von aus der Schmelze gezüchteten Kristallen in den Systemen Kupfer-Indium-Selen und Kupfer-Indium-Gallium-Selen für photovoltaische Anwendungen, Shaker Verlag (1999)

[49] H. Dittrich, U. Prinz, J. Szot, H. W. Schock, Analysis of reaction kinetics of selenized $CuInSe_2$ and $CuGaSe_2$ thin films, Proc. 9th EC Photovoltaic Solar Energy Conf. (1989) 163-166

[50] S. Kim, W.K. Kim, R. M. Kaczynski, R.D. Acher, S. Yoon, T.J. Anderson, O. D. Crisalle, E.A. Payzant, S.S. Li, Reaction kinetics of $CuInSe_2$ thin films grown from bilayer InSe/CuSe precursors, J. Vac. Sci. Techn. A Vacuum, Surfaces, Films 23 (2005) 310-315

[51] W. K. Kim, E.A. Payzant, S. Kim, S.A. Speakman, O. D. Crisalle, T.J. Anderson, Reaction kinetics of $CuGaSe_2$ formation from a GaSe/CuSe bilayer precursor film, J. Cryst. Growth 310 (2008) 2987–2994

[52] Polyxeni Tsoulka, Adrien Rivalland, Ludovic Arzel, Nicolas Barreau, Improved $CuGaSe_2$ absorber properties through a modified co-evaporation process, Thin Solid Films (2020), “accepted”

[53] Polyxeni Tsoulka, Local inhomogeneities in polycrystalline wide band gap $CuIn_{1-x}Ga_xSe_2$ thin-films, PhD Thesis, Nantes (2019)

[54] M. Marudachalam, R.W. Birkmire, H. Hichri, J.M. Schultz, A. Swartzlander, M.M. Al-Jassim, Phases, morphology, and diffusion in $CuIn_xGa_{1-x}Se_2$ thin films, J. Appl. Phys. 82 (1997) 2896-2905

[55] N. Barreau, T. Painchaud, F. Couzine-Devy, L. Arzel, J. Kessler, Recrystallization of CIGSe layers grown by three-step processes: A model based on grain boundary migration, Acta Mater. 58 (2010) 5572-5577

[56] F. Couzinie-Devy, N. Barreau, J. Kessler, Re-investigation of preferential orientation of Cu(In,Ga)Se_2 thin films grown by the three-stage process, Prog. Photovolt: Res. Appl. 19 (2011) 527-536

[57] J. Kessler, C. Chityuttakan, J. Lu, J. Schöldström, L. Stolt, Cu(In,Ga)Se_2 Thin films Grown with a Cu-Poor/Rich/Poor Sequence: Growth model and structural considerations, Prog. Photovolt: Res. Appl. 11 (2003) 319-331

[58] G. Hanna, J. Mattheis, V. Laptev, Y. Yamamoto, U. Rau, H.W. Schock, Influence of the selenium flux on the growth of Cu(In,Ga)Se_2 thin films, Thin Solid Films 431–432 (2003) 31–36

[59] N. Ott, G. Hanna, U. Rau, J.H. Werner, H.P. Strunk, Texture of Cu(In,Ga)Se_2 thin films and nanoscale cathodoluminescence, J. Phys. Condens. Matter 16 (2004) 85-89

[60] S. Ishizuka, A. Yamada, P.J. Fons, H. Shibata, S. Niki, Structural tuning of wide-gap chalcopyrite $CuGaSe_2$ thin films and highly efficient solar cells: differences from narrow-gap Cu(In,Ga)Se_2, Prog. Photovolt. Res. Appl. 22 (2013) 821-829

[61] V. Deprédurand, T. Bertram, D. Regesch, B. Henx, S. Siebentritt, The influence of Se pressure on the electronic properties of $CuInSe_2$ grown under Cu excess, Appl. Phys. Lett. 105 (2014) 172104

[62] M. Marudachalam, H. Hichri, R. Klenk, R.W. Birkmire, W.N. Shafarman, J. M. Schultz Preparation of homogeneous Cu(In,Ga)Se_2 films by selenization of metal precursors in H_2Se atmosphere Appl. Phys. Lett. 67 (1995) 3978-3980

List of figures

List of tables

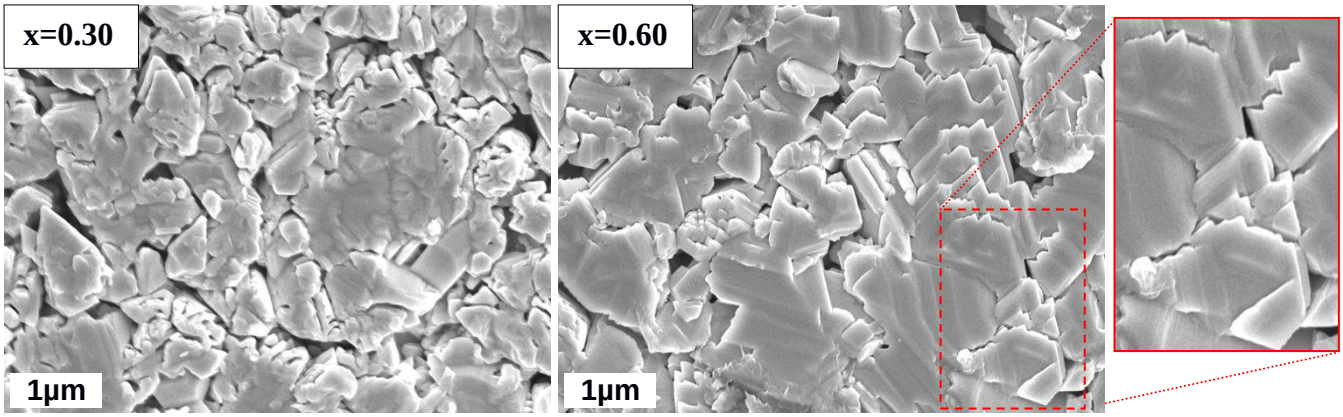

Figure 1: *SEM surface images of the CIGSe layers: #01 with x=0.30 (left) and #02 with x=0.60 (right) without post-deposition treatment*

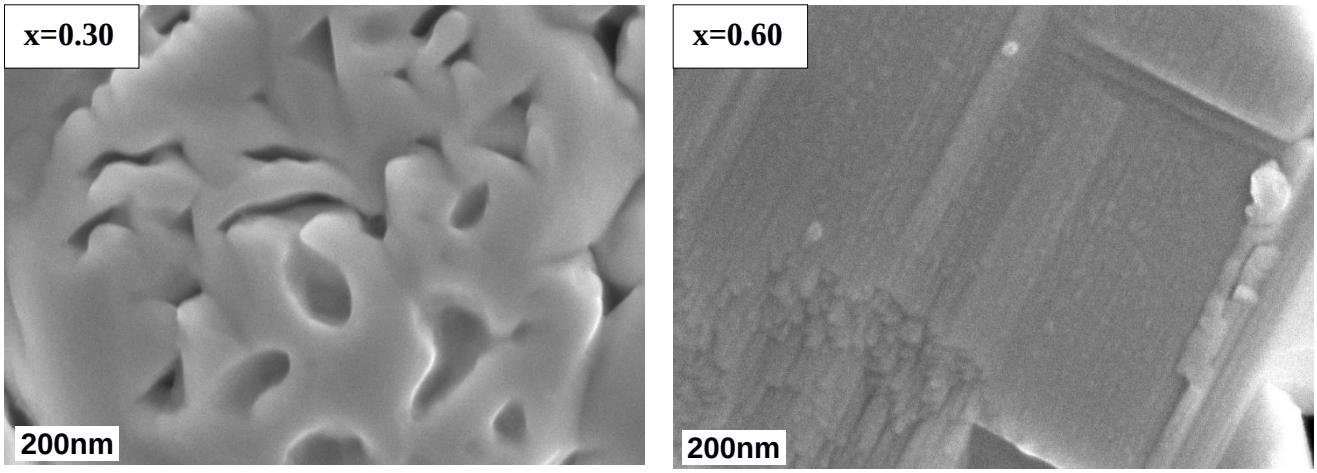

Figure 2: *SEM surface images of CIGSe films, after the KCN surface etching and annealing under vacuum: #01 with x=0.30 (left) and #02 with x=0.60 (right)*

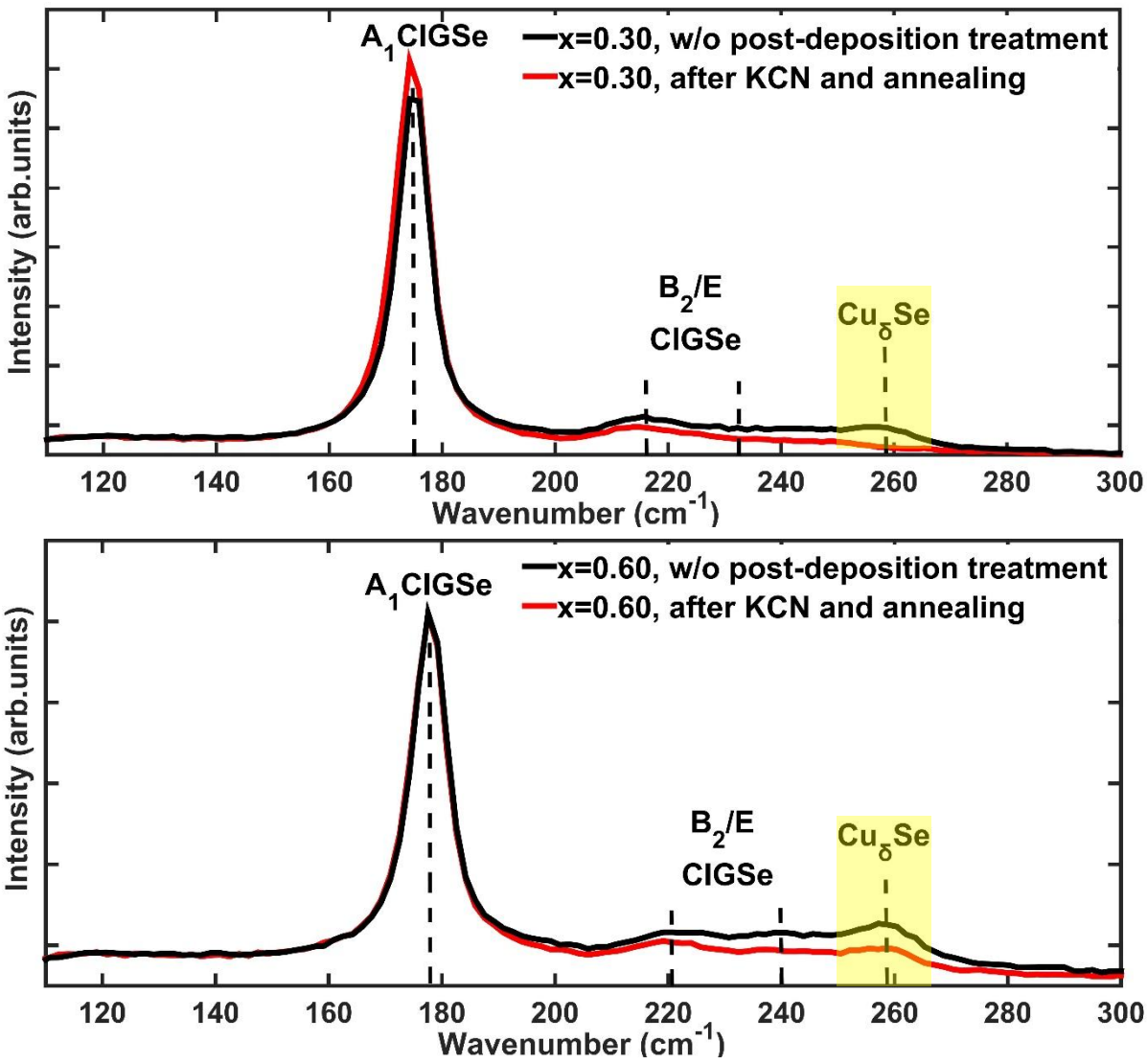

Figure 3: Raman analysis of the CIGSe films #01 with x=0.30 (a) and #02 with x=0.60 (b). The black lines correspond to the Raman spectra of the samples without any post-deposition treatment. The red lines represent the samples after the KCN etching and annealing. The peak that corresponds to the copper selenide phase is highlighted in yellow

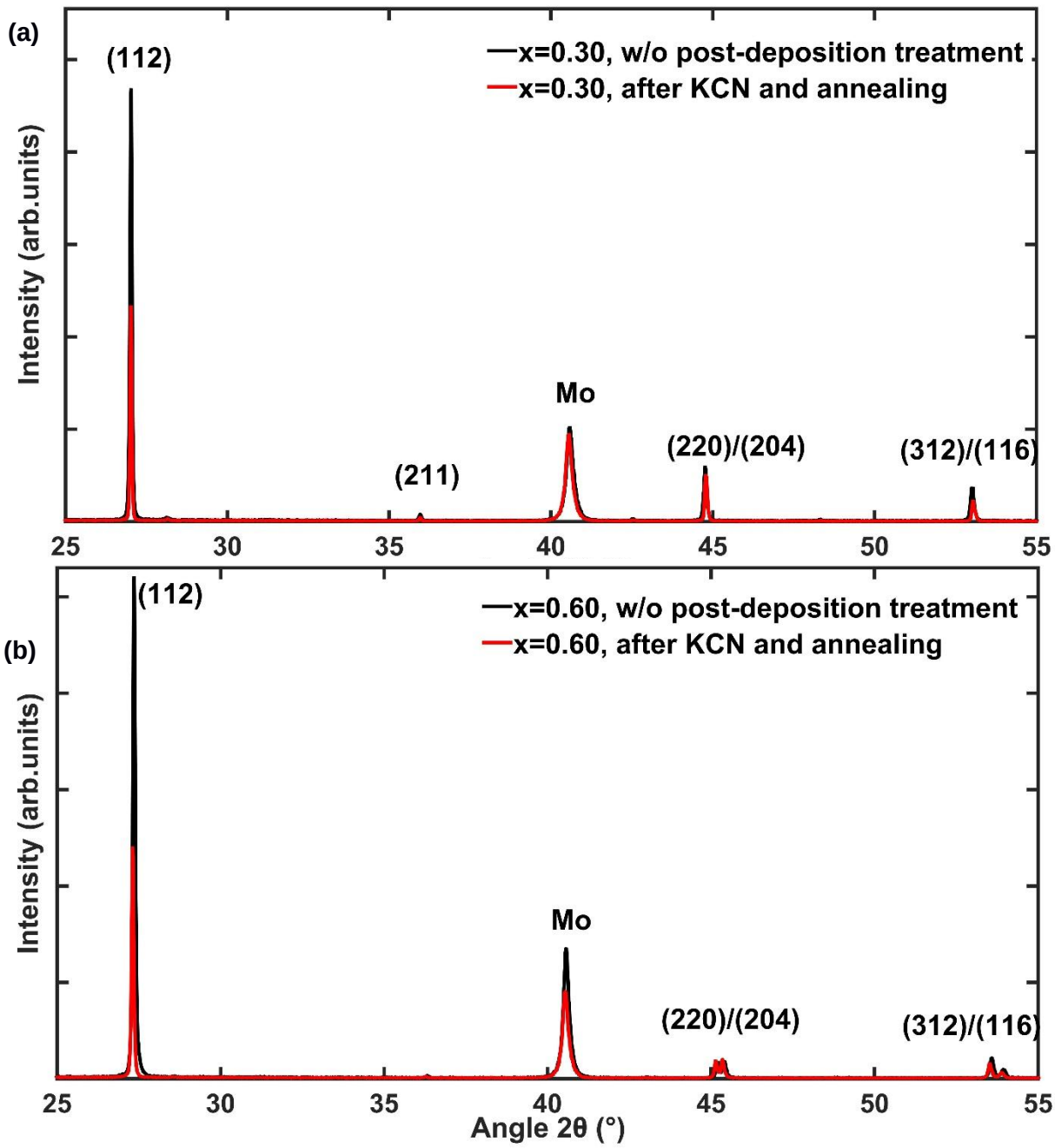

Figure 4: *XRD analysis of x=0.30 (#01, (a)) and x=0.60 (#02, (b)) CIGSe layers grown on SLG/SiN/Mo. The black lines illustrate the diffractogram of the final CIGSe layers obtained after the end of the two-stage co-evaporation process and they did not undergo any post-deposition process. The red lines show the diffractogram obtained for the CIGSe samples after the KCN surface etching and annealing under vacuum for 30 days at 350°C*

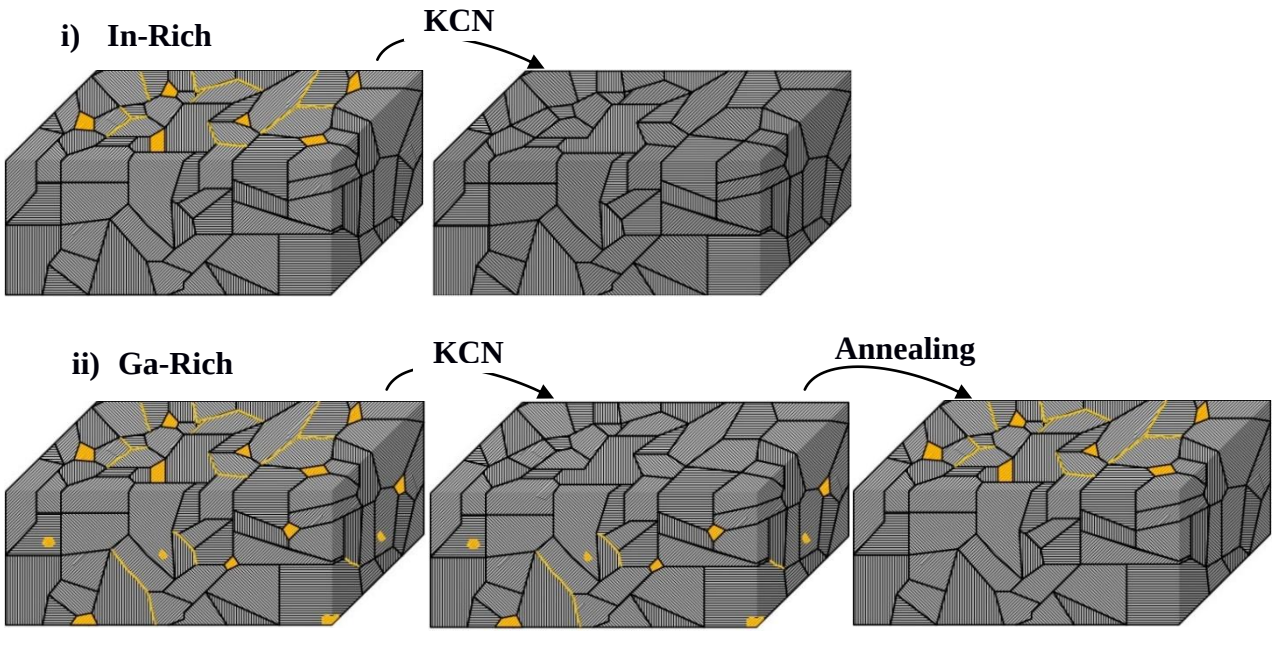

Figure 5: *Schematic representation of the copper selenide surface segregation and bulk precipitation in the case of i) In-rich CIGSe and ii) Ga-rich CIGSe absorber layers. At the In-rich sample after the end of the CIGSe growth the copper selenide has entirely segregate at the surface of the film. Hence the removal of the copper selenide phases from the surface leaves a homogeneous CIGSe film without any detrimental Cu-rich secondary phases. At the Ga-rich sample, the duration of the deposition process is not sufficient to homogenize the film and make the copper selenide compounds segregate at the surface. As a result, after the end of the deposition process, there are Cu-enriched bulk precipitates within the bulk of the absorber layer, that they cannot be removed by the KCN treatment. A long annealing under vacuum is then required for the Ga rich absorber to make the entire $Cu_{\delta}Se$ segregate at the surface*

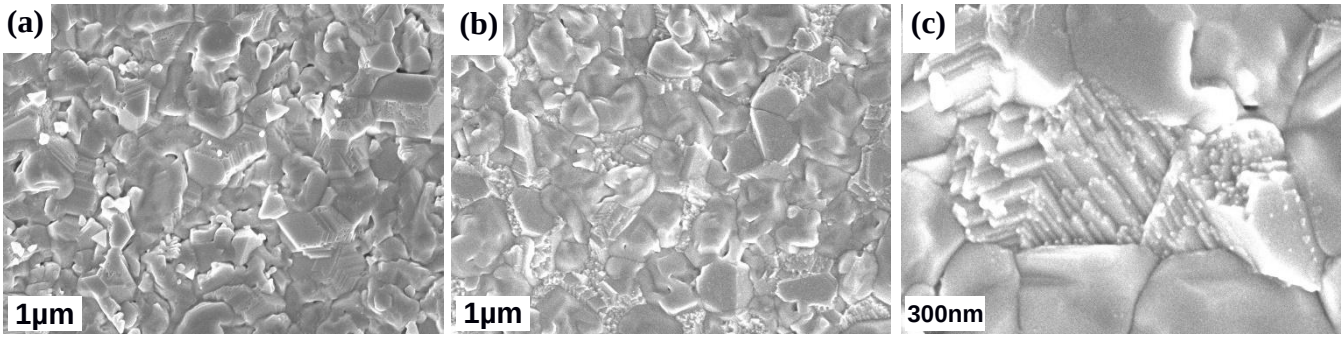

Figure 6: *SEM surface images of CGSe Cu-rich layer (#03) deposited on Mo, (a) after the co-evaporation without post-deposition treatment, (b) after annealing at 350°C for 24h under vacuum and (c) high-magnification image of the sample after annealing at 350°C for 24h*

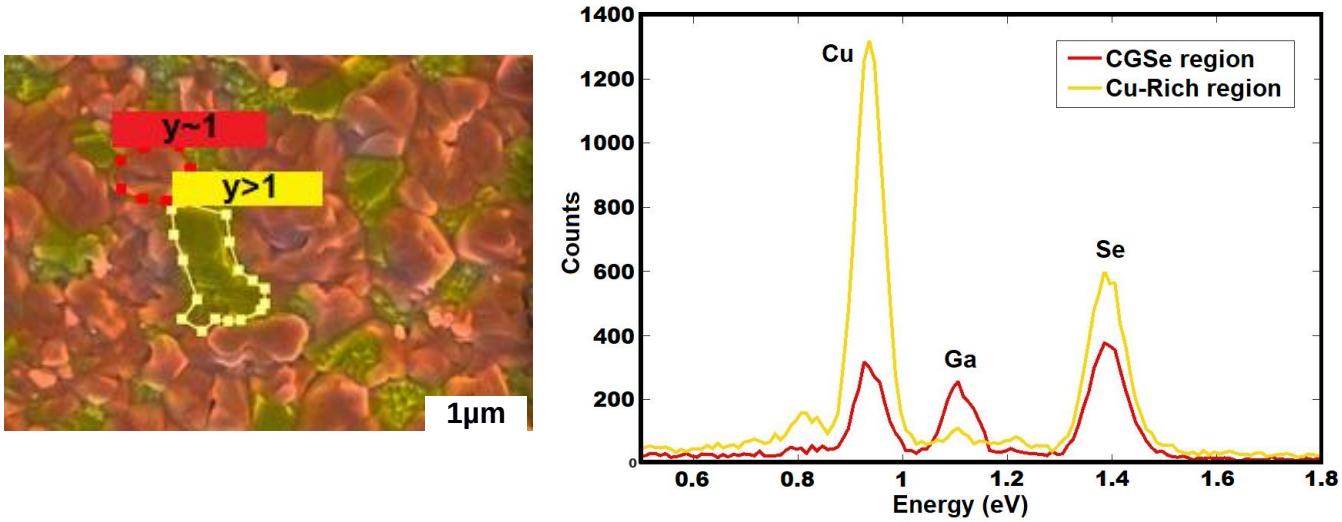

Figure 7: *Left: SEM surface image coupled with EDS surface cartography (at 5kV acceleration voltage) of the In-free CGSe film (#03) after annealing. Right: The elemental concentration of the two grains highlighted by the dotted circles in the SEM image. The red curve in the EDS spectrum corresponds to a stoichiometric CGSe region while the yellow curve represents a Cu-enriched region and the presence of copper selenide secondary phases*

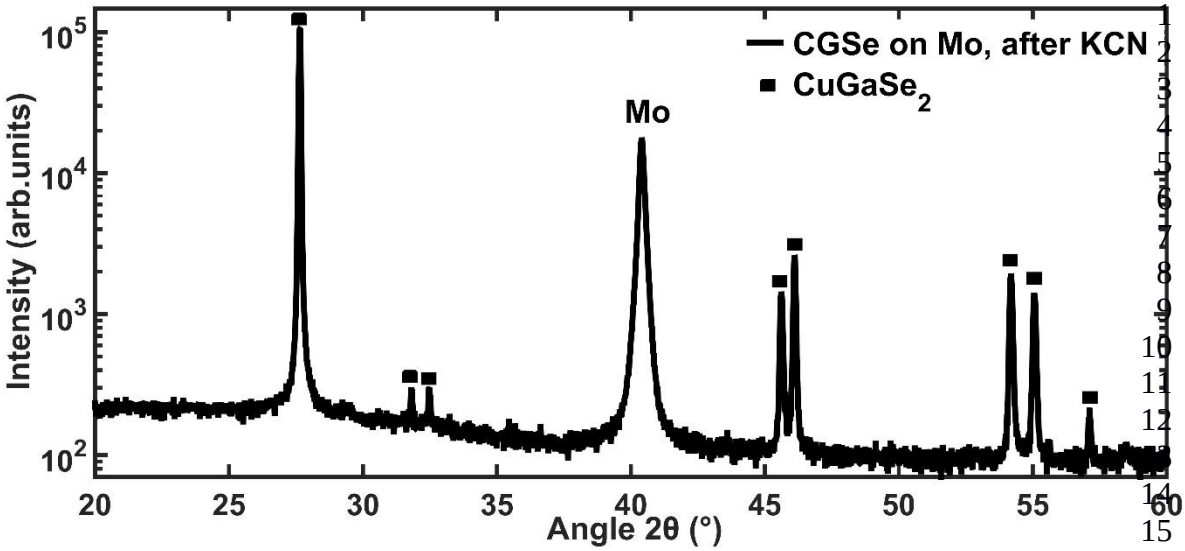

Figure 8: XRD analysis *of a CGSe sample (#04, y=0.95) grown on SLG/Mo by two-stage co-evaporation process (Cu-RO). The diffractogram does not present any $Cu_{\delta}Se$ peak. The y axis represents the logarithm of the intensity*

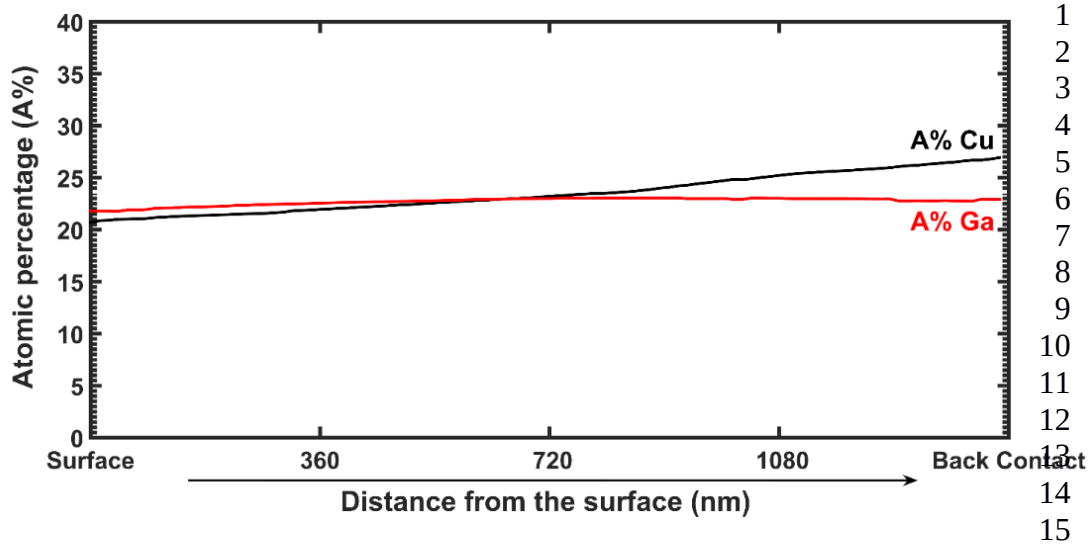

Figure 9: *SEM-EDS cross-section elemental profile of a CGSe sample (#04, y=0.95) grown on Mo by a two-stage co-evaporation process (Cu-RO). The EDS measurement was performed at 10 kV beam acceleration voltage*

Table I: *Summary of the elemental concentration x=[Ga]/([Ga]+[In]) and y=[Cu]/([Ga]+[In]) measured by EDS at 20 kV acceleration voltage, the substrate, the CIGSe co-evaporation process and the post-deposition treatment (KCN etching and annealing) of each sample. The y_R, y and y_A denote the Cu content at the end of the Cu-rich stage, after the end of the co-evaporation process and after the annealing respectively. The error at the atomic percentage is ±0.03*

sample	x	y_R	y	y_A	Substrate	Co-evaporation process	KCN etching	Annealing[1]
#01	0.30	1.36	0.98	0.92	SLG/ Si_xN /Mo	Cu-RO	YES	30 days
#02	0.60	1.39	0.87	0.86	SLG/ Si_xN /Mo	Cu-RO	YES	30 days
#03	1.00	-	1.50	-	SLG/Mo	Cu-R	NO	24 hours
#04	1.00	-	0.95	-	SLG/ Mo	Cu-RO	YES	-

[1]For the annealing of 30 days the samples were sealed under vacuum in quartz tubes. The annealing of 24 hours was carried out in a chamber under vacuum